Chinese Journal of Catalysis 42 (2021) 1216–1226

available at www.sciencedirect.com

ScienceDirect

journal homepage: www.sciencedirect.com/journal/chinese-journal-of-catalysis

Article

Enhancing the activity, selectivity, and recyclability of Rh/PPh_3 system-catalyzed hydroformylation reactions through the development of a PPh_3-derived quasi-porous organic cage as a ligand

Wenlong Wang [b,†], Cunyao Li [a,†], Heng Zhang [c,†], Jiangwei Zhang [a], Lanlu Lu [d], Zheng Jiang [d,e], Lifeng Cui [b], Hongguang Liu [c,#], Li Yan [a,$], Yunjie Ding [a,*]

[a] *Dalian National Laboratory for Clean Energy, and State Key Laboratory of catalysis, Dalian Institute of Chemical Physics, Chinese Academy of Sciences, Dalian 116023, Liaoning, China*

[b] *School of Materials Science and Engineering, Dongguan University of Technology, Dongguan 523808, Guangdong, China*

[c] *College of Chemistry and Materials Science, Jinan University, Guangzhou 510632, Guangdong, China*

[d] *Shanghai Advanced Research Institute, Chinese Academy of Sciences, Shanghai 201210, China*

[e] *Shanghai Synchrotron Radiation Facility, Shanghai Institute of Applied Physics, Chinese Academy of Sciences, Shanghai 201204, China*

ARTICLE INFO

Article history:
Received 22 October 2020
Accepted 25 November 2020
Available online 5 March 2021

Keywords:
Hydroformylation
Triphenylphosphine
Porous organic cages
Chemical selectivity
Linear-regioselectivity

ABSTRACT

In contrast to heterogeneous network frameworks (e.g., covalent organic frameworks and metal-organic frameworks) and porous organic polymers, porous organic cages (POCs) are soluble molecules in common organic solvents that provide significant potential for homogeneous catalysis. Herein, we report a triphenylphosphine-derived quasi-porous organic cage (denoted as POC-DICP) as an efficient organic molecular cage ligand for Rh/PPh_3 system-catalyzed homogeneous hydroformylation reactions. POC-DICP not only displays enhanced hydroformylation selectivity (aldehyde selectivity as high as 97% and a linear-to-branch ratio as high as 1.89) but can also be recovered and reused via a simple precipitation method in homogeneous reaction systems. We speculate that the reason for the high activity and good selectivity is the favorable geometry (cone angle = 123.88°) and electronic effect (P site is relatively electron-deficient) of POC-DICP, which were also demonstrated by density functional theory calculations and X-ray absorption fine-structure characterization.

1. Introduction

Researchers in the field of catalysis have made considerable effort to search for new porous materials over the past decades, as porous materials play critical roles in catalytic processes, such as those of adsorption, mass transfer, and diffusion [1].

* Corresponding author. Tel/Fax: +86-411-84379143; E-mail: dyj@dicp.ac.cn
# Corresponding author. Tel: +86-15602302185; E-mail: hongguang_liu@jnu.edu.cn
$ Corresponding author. Tel/Fax: +86-411-84379143; E-mail: yanli@dicp.ac.cn
† These authors contributed equally to this work.

This work was supported by the Strategic Priority Research Program of the Chinese Academy of Sciences (XDB17020400, XDA21020300), the National Key R&D Program of China (2017YFB0602203), National Natural Science Foundation of China (21972018), Dongguan University of Technology (DGUT) Research Center of New Energy Materials (KCYCXPT2017005) and the Startup Research Fund of DGUT (KCYKYQD2017015).
DOI: 10.1016/S1872-2067(20)63746-9 | http://www.sciencedirect.com/journal/chinese-journal-of-catalysis | Chin. J. Catal., Vol. 42, No. 7, July 2021

Long-range-ordered metal-organic frameworks (MOFs) [2–8] and covalent organic frameworks (COFs) [9–13] and amorphous porous organic polymers (POPs) [14–20] have been extensively examined in catalysis for their favorable pore structures during the last decade. Nevertheless, very little attention has been paid to molecular porous organic cages (POCs) [21–30], whose concept was formally raised by Cooper *et al*. [21] in 2009. POCs are porous molecular materials built from discrete organic cage molecules. In contrast to heterogeneous network porous frameworks (COFs and MOFs) and POPs, POCs are soluble molecules in ordinary organic solvents, whose advantages not only include the generally porous nature of heterogeneous catalysts but also the significant potential for homogeneous catalysis.

In principle, POCs can be judiciously designed and synthesized by covalently assembling two differently shaped molecular building blocks (BBs) as components of three-dimensional (3D) polycyclic cage molecules, which are represented by topologies of Archimedean and Platonic solids [31,32]. However, compared with well-developed and mature MOF, COF, and POP materials, the combinational requirements of porous crystal packing [21,33], shape persistence, and the synthetic challenge of functionalized BBs make functional POC molecules easy to design but relatively harder to synthesize. In fact, only a few POCs with catalytic functionality have been reported. To our knowledge, the research groups of Chang and Kim reported porphyrin-functionalized POCs for electrochemical CO_2 reduction catalysis [34,35]. Xu *et al*. [36,37] and Dong *et al*. [38] elucidated the encapsulation of highly catalytically active metal nanoclusters inside POCs. Wang and co-workers reported POC-stabilized Pd nanoparticles (NPs) as efficient heterogeneous catalysts for the carbonylation reaction of aryl halides [39]. Mukherjee et al. [40] developed molecular-cage-supported Pd NPs as an additive-free and efficient heterogeneous catalyst for the cyanation reaction of aryl halides. Beaumont et al. [41] also reported POC-supported Pd NPs as catalysts for CO oxidation. For other functional POCs, please see references [42–52]. However, note that these are not catalytic functionalities.

Catalytic hydroformylation is one of the most significant reactions in the fine chemical industry [53–60], which can be traced back to Otto Roelen's discovery during the period of his study of F-T synthesis in 1938 [61]. At the present time, in excess of 10 million metric tons of alcohols and aldehydes are produced every year [53]. Owing to its long history and large production scale, the hydroformylation reaction has been recognized as a "pioneer of industrial homogeneous catalysis". Triphenylphosphine (PPh_3) is one of the most classical organophosphorus ligands, widely used in the area of catalysis and organometallic chemistry. Among the various developed catalysts for hydroformylation reactions, the Rh/PPh_3 (ligand) system is one of the most efficient catalytic systems and has been widely used in both industry and academic research. For example, the Wilkinson catalyst ($RhCl(PPh_3)_3$), which was invented in 1965, played a vital role in the history of catalytic hydroformylations [62,63]; however, the recycling of the Wilkinson catalyst remains a large problem, especially for long-chain olefin hydroformylations, as long-chain aldehydes usually have high boiling points, and the Wilkinson catalyst decomposes easily during distillation. Another well-known case is the biphasic Ruhrchemie/Rhone-Poulenc process, which employs sulfonated phosphine ligand TPPTS (Fig. 1) to realize the separation of the Rh/P catalyst and aldehyde products [64–66]. This aqueous two-phase propene hydroformylation is the only aqueous two-phase technology in industry to date since 1984. Regrettably, long-chain olefin hydroformylation cannot react efficiently through the Ruhrchemie/Rhone-Poulenc method because of the phase-transfer limitations arising from the poor solubility of various long-chain olefin substrates in water.

Based on the above facts as well as the progress of our long-standing research efforts in hydroformylation [67–74], herein, we introduce a PPh_3-based new-generation hydroformylation cage-type ligand (denoted as POC-DICP) as a recyclable and efficient catalyst for long-chain olefin hydroformylation reactions (Fig. 2). The combined advantages of solubility, a large steric effect, and favorable electron effect make POC-DICP an attractive ligand in homogeneous catalysis, as the catalytic selectivity is enhanced through the influence on the reaction transition state by favorable steric hindrance and electron effects. It should be mentioned that the POC-DICP ligand is assembled together by two PPh_3 and three cyclohexanediamine moieties through imine bonds. We found that imine products with two or more imine bonds are usually insoluble in methanol, providing an opportunity for homogeneous catalysis and heterogeneous separation; this system represents a homogeneous catalytic system using a Rh/POC-DICP catalyst. After the reaction, methanol was added dropwise to precipitate the POC catalyst and realize heterogeneous separation. This type of homogeneous catalysis and heterogeneous separation tactic represents an elegant and advanced methodology in the area of catalyst recycling, which not only maintains the high catalytic activity and selectivity but also attains the goal of catalyst recycling. This is an advantage that traditional immobilized catalysts (heterogenized homogeneous catalysts) do not have [75]. Catalytic hydroformylation reactions with significant impact, including various liquid-phase high-carbon olefin hydroformylations, have been employed to investigate the effectiveness and practicability of our strategy for POC ligand-assisted catalysis. To conduct in-depth studies, Rh K-edge X-ray absorp-

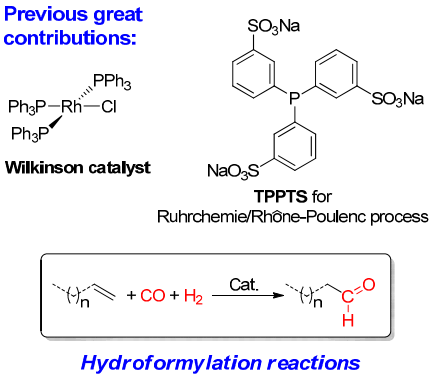

Fig. 1. Famous Rh/PPh_3 catalytic systems for hydroformylation reaction.

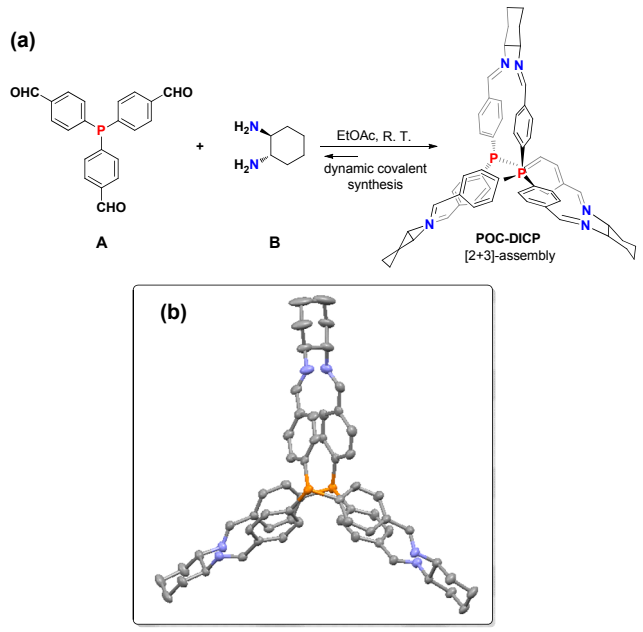

Fig. 2. (a) Synthesis of PPh_3-derived POC by dynamic covalent synthesis (b) single crystal structure determined by X-ray diffraction (for clarity, H atoms are omitted), CCDC number: 1857136.

tion fine structure (EXAFS and XANES) spectra and detailed density functional theory (DFT) calculations were implemented to reveal the fundamental merit and trustable mechanism of our cage ligand-based hydroformylations.

2. Experimental

2.1. Materials

All reagents were purchased and used directly without further purification. Here, (*s*,*s*)-1,2-cyclohexanediamine (Alfa Aesar Co., Ltd.), 4-bromobenzaldehyde diethyl acetal (Energy Chemical Co., Ltd.), phosphorus trichloride (Energy Chemical Co., Ltd.), and dicarbonyl (2,4-pentanedionato)rhodium(I) (Alfa Aesar Co., Ltd.) were acquired. All the olefins were purchased from J&K Scientific. Co., Ltd.

2.2. Characterization methods

Liquid nuclear magnetic resonance (NMR) spectra were recorded on a Bruker AVANCE III NMR spectrometer at 100 MHz for ^{13}C spectra and 400 MHz for ^{1}H spectra. Chemical shifts were reported as δ values in ppm relative to the deuterated solvent peak ($CDCl_3$, δ_C: 77.16; δ_H: 7.26). The electrospray ionization high-resolution mass spectra (ESI-HRMS) data were collected via an Agilent Q-TOF6540 spectrometer. Single crystal X-ray diffraction (SXRD) data were collected on an Agilent GeminUltra diffractometer with Mo K_α radiation, and liquid-nitrogen purging was needed to prevent crystal cracking. Morphological characterization was performed using helium ion microscopy (HIM) from Carl Zeiss ORION NANOFAB. The nitrogen adsorption test was carried out on a Quantachrome Autosorb-1 instrument at 77 K.

2.3. Synthesis of POC-DIPC

Ethyl acetate (150 mL) was added to PPh_3-based trialdehyde (**A**, 429 mg, 1.24 mmol) [76] in a beaker at room temperature (Fig. 1(a)). The suspension was stirred with a glass rod and clarified. Next, a solution of (*s*,*s*)-1,2-cyclohexanediamine (**B**, 212 mg, 1.86 mmol) in ethyl acetate (30 mL) was added dropwise, and a turbid solution was observed during the addition process. The resulting mixture was left covered for 72 h without stirring. Precipitation was observed in approximately 1–2 h. After the reaction, the resulting mixture was filtered, and the filtrate was concentrated to approximately 5 mL using a rotary evaporator. After the addition of methanol (100 mL) to the filtrate, the product was slowly precipitated as a white powder. The final cage product (79% yield, 454 mg) was collected by filtration and dried under reduced pressure.

^{1}H NMR ($CDCl_3$, 400 MHz): δ (ppm) = 7.67 (s, 6H), 7.30 (d, 12H, J = 4.0 Hz), 6.99 (t, 12H, J = 8.0 Hz), 3.19 (t, 6H, J = 8.0 Hz), 2.13 (d, 6H, J = 12.0 Hz), 1.92 (d, 12H, J = 8.0 Hz), 1.51 (t, 6H, J = 8.0 Hz); ^{13}C NMR ($CDCl_3$, 100 MHz): δ (ppm) = 163.1, 139.1, 139.0, 136.6, 133.2, 133.1, 127.7, 127.6, 73.2, 32.0, 24.4; ^{31}P NMR ($CDCl_3$, 400 MHz): δ (ppm) = −7.8; HRMS (ESI): m/z calc. for $[C_{60}N_6P_2H_{60}]$: 926.4355; found 927.4460 $[M+H]^+$.

2.4. Procedures for the catalytic hydroformylations of high olefins

A stainless batch-tank reactor loaded with a magnetic stirrer was used to perform the reactions. As a representative run, 13.8 mg of POC-DICP ligand, $Rh(CO)_2(acac)$ (0.384 mg, 38.4 mg of $Rh(CO)_2(acac)$ was dissolved in 100 mL toluene to prepare a stock solution, and 1 mL stock solution was added), 1-octene (2 g), and toluene (5 mL) were added to the reactor, substrate/catalyst = 12000. The reactor was then sealed and purged with syngas (H_2/CO = 1:1) 3 times, and the initial pressure of syngas was regulated to 1 MPa. Then, the reactor was heated to 100 °C (within 30 min) and stirred for 4 h at a stirring speed of 300 r/min. After the reaction was completed, the reactor was cooled to ambient temperature, and the excess syngas was vented. The solution was analyzed by GC (Agilent 7890A loaded with an HP-5 column, *n*-butanol was used as an internal standard.

2.5. Procedures for the catalytic hydroformylation of propene

A stainless batch-tank reactor loaded with a magnetic stirrer was used to perform the reaction. First, 13.8 mg of POC-DICP ligand, $Rh(CO)_2(acac)$ (0.384 mg, 38.4 mg of $Rh(CO)_2(acac)$ was dissolved in 100 mL toluene to prepare a stock solution, and 1 mL stock solution was added), and toluene (5 mL) were added to the reactor. Then, the reactor was sealed and purged with a gas mixture (propene/CO/H_2 = 1:1:1) three times, and the initial pressure of the gas mixture (propene, CO, and H_2) was adjusted to 1.5 MPa. Finally, the reactor was heated to 100 °C (within 30 min) and stirred for 4 h at a stirring speed of 300 r/min. After the reaction was completed, the reactor was cooled to ambient temperature, and the excess

gas mixture was vented. The solution was analyzed by gas chromatography (GC) (Agilent 7890A loaded with an HP-5 column, n-butanol was used as an internal standard).

2.6. Rh K-edge X-ray absorption fine structure (EXAFS and XANES) spectra

EXAFS and XANES spectra of the catalysts were acquired at the BL14W1 beamline (SINAP, Shanghai, China), and a Si(311) crystal monochromator was used. The storage ring was operated at 3.5 GeV, and the injection current was 200 mA. An Rh foil was applied as a reference sample, and all the X-ray absorption spectra were tested in transmission mode. All spectra of the as-synthesized catalysts were obtained in fluorescence mode. The raw data were energy-calibrated (Rh K-edge energy of Rh foil) at 23 220 eV, the first inflection point. Then, they were background-corrected and normalized using IFEFFIT software. A Fourier transformation of the EXAFS data was used for the k3-weighted functions. For the curve-fitting analysis, Rh-P and Rh-C path parameters were obtained from the ab initio multiple scattering codes FFEF6.

2.7. Synthesis of pre-catalyst that was used as a sample for EXAFS test

A 100 mL stainless autoclave was loaded with $Rh(CO)_2(acac)$ (3.84 mg), POC-DICP (138 mg), and toluene (50 mL). The reactor was then sealed and purged with syngas (H_2/CO = 1:1) three times, and the initial pressure of syngas was regulated to 1 MPa. Then, the reactor was heated to 100 °C (within 30 min) and stirred for another 30 min at a stirring speed of 300 r/min. After the reaction was completed, the autoclave was cooled to ambient temperature, and the excess syngas was vented. The mixture was then evaporated under reduced pressure to remove the toluene. The crude product was washed with methanol (20 mL × 3) to obtain the pre-catalyst that was used for the EXAFS test.

2.8. Catalyst recycling experiments in high olefin hydroformylations

As a representative run, POC-DICP ligand (69.0 mg), $Rh(CO)_2(acac)$ (3.84 mg), 1-octene (20.0 g), and toluene (50 mL) were added to the autoclave, substrate/catalyst = 12000. The reactor was then sealed and purged with syngas (H_2/CO = 1:1) 3 times, and the initial pressure of syngas was regulated to 1 MPa. Then, the autoclave was heated to 100 °C (within 30 min) and stirred for 4 h. The stirring speed was 420 r/min, and the pressure was adjusted by a pressure-regulating valve to maintain a pressure of 1 MPa. After the reaction was completed, the autoclave was cooled to ambient temperature, and the excess syngas was vented. The mixture was analyzed by GC. The mixture was then evaporated under reduced pressure to remove the toluene. Then, methanol (200 mL) was added to the system to precipitate the catalyst. The catalyst was separated by centrifugation and reused for the next run.

2.9. Computational details

All quantum mechanical calculations were conducted by employing DFT with the Gaussian 09 package. Structures were optimized using the B3LYP functional without any constraints in the solvent phase. The SMD solvent model [77] was utilized, and toluene was chosen as the solvent. The 6-31G(d,p) basis set was used for all elements except for Rh, for which the LANL2DZ basis set and pseudopotential were employed with an extra f-polarization function (ξ_f = 1.350) [78] Vibrational frequency calculations at the same level were performed to verify that each stationary point was either a minimum (no imaginary frequency) or a transition state (only one imaginary frequency). Intrinsic reaction coordinate calculations were conducted to verify the transition-state structures. Single-point calculations were performed at a higher theoretical level, M06-L, with a def2-TZVP basis set and pseudopotential for Rh, and a 6-311+G(d,p) basis set was adopted for all the other atoms to determine the free energies for use at the B3LYP-optimized geometries. Empirical D3 dispersion corrections were included for the M06-L functional [79].

3. Results and discussion

3.1. Design and synthesis of POC-DICP

First, a new and significant molecular building block of PPh_3-based trialdehyde (A) was designed and successfully synthesized (for detailed synthetic procedures, see Section 2.3). With this important building block in hand, the [2 + 3] imine cage POC-DICP was afforded through "dynamic covalent chemistry" [26,29] (Fig. 2(a)), of which the advantages are the thermodynamic structural error self-correction mechanism and its resulting relatively high yields (79% isolated yield in this case). It is worth noting that the crystalline product was obtained by recrystallization, which could be further grown to large-grained single crystals suitable for X-ray single crystal diffraction.

3.2. Characterization of POC-DICP

The cage is soluble in ordinary organic solvents, such as ethyl acetate, CH_2Cl_2, $CHCl_3$, DMF, and toluene. Therefore, ESI-HRMS could be directly employed to determine the accurate molecular weight information, and in this case, ESI-HRMS analysis showed $[M + H]^+$ molecular ions at m/z = 927.4460, corresponding to [2 + 3] (6 imine bond formation) condensation stoichiometry (Fig. 2(a)). Furthermore, owing to the solubility of the cage in $CDCl_3$, liquid NMR could also be used to determine the structural information of the cage, as the ^1H, ^{13}C, and ^{31}P NMR confirmed the molecular structure illustrated in Fig. 2(a).

To identify the 3D structure of the cage molecule directly, the SXRD method was introduced after the growth of large-grained single crystals. Crystals suitable for SXRD were obtained by the slow diffusion of methanol to the CH_2Cl_2 solution of the cage molecule. It is worth noting that the crystals

become opaque and crack within seconds in air; thus, protective paraffin oil and the purging of liquid nitrogen are needed during the diffraction data collection process. The 3D molecular structure is illustrated in Fig. 2(b). Two triphenylphosphine-based trialdehyde molecules and three cyclohexanediamine molecules were assembled into a 3D cage molecule. The cage POC-DICP was crystallized in the monoclinic space group C2 (a = 20.0305 Å, b = 23.4203 Å, c = 25.8132 Å, $\alpha = \gamma = 90°$, β = 98.089°, V = 11989.0 Å^3) with two crystallographically independent molecules. To further investigate the particulate morphology and physical form of the cage material, HIM was employed to observe the sample obtained after recrystallization (Figs. 3(a–d)). Regular micron-sized plate crystals conglomerate together to form beautiful nanoflowers. All of this evidence suggests that our cage material has good crystallinity.

The nitrogen gas sorption experiment was carried out at 77 K to investigate the pore structure of the cage material POC-DICP (Fig. 4). Before the analysis, the cage material was degassed with a turbo molecular pump at 180 °C for 10 h. The measured isotherm seems a bit strange compared with the known isotherm types, and the adsorption and desorption branches did not close. Moreover, there was no micropore filling step, which indicated that the pores of the cage material were mainly mesopores that were generated by the accumulation of each single microcrystalline cage. In view of this, calculating the pore size distribution curve (using the NLDFT method) and BET surface area may be unreliable in this case. Therefore, the pore size distribution information and BET surface area are not provided here. Transmission electron microscopy (TEM) images show the existence of mesopores (see Supporting Information), which can be attributed to the cage-cage packing effect. In view of this, we named our cage material a quasi-porous organic cage.

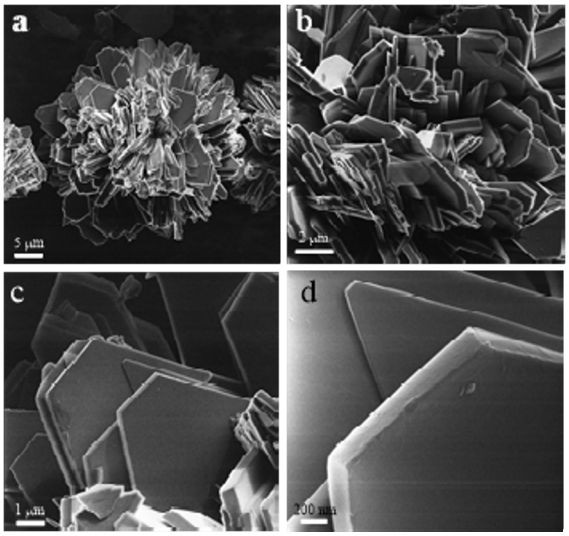

Fig. 3. Morphological characterization of POC-DICP by helium ion microscopy. (a) Scale bar = 5 μm; (b) Scale bar = 2 μm; (c) Scale bar = 1 μm (d) Scale bar = 200 nm.

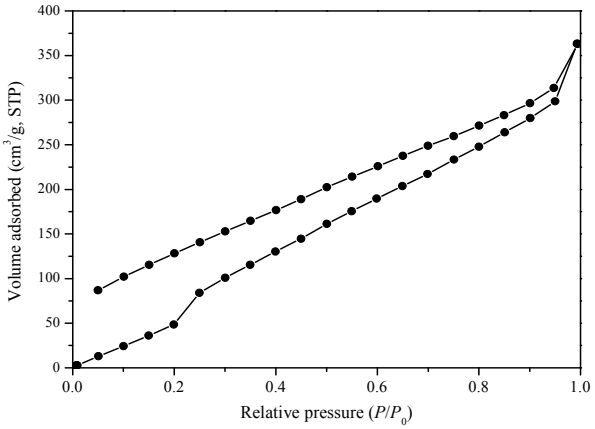

Fig. 4. Nitrogen gas sorption isotherm at 77 K for cage POC-DICP.

3.3. *Catalytic liquid-phase hydroformylations of high olefins*

The reaction data were satisfactory for the performance of a series of control experiments, and the ligand POC-DICP displayed high activity and selectivity compared with the classical PPh_3 ligand. First, the catalytic hydroformylation activities of 1-octene employing different catalysts were examined (Table 1). For a substrate/catalyst (S/C) = 12000, the reaction time was 1 h, the homogeneous Rh/POC-DICP catalyst displayed high conversion (97.8%), aldehyde selectivity was moderate (59.8%), and the regioselectivity of aldehydes (linear-to-branch ratio, l/b) was 1.46 (Table 1, entry 1). We then compared our catalyst with classical PPh_3-assisted Rh catalysts. When the homogeneous Rh/PPh_3 catalyst was used (Table 1, entry 2), the aldehyde selectivity decreased from 59.8% to 37.2%, and the iso-alkene selectivity increased from 37.4% to 57.4%. When the reaction time was increased to 4 h, the aldehyde selectivity of the Rh/POC-DICP catalyst was increased to 88.9% (Table 1, entry 3); however, the aldehyde selectivity of Rh/PPh_3 was only 53.3% (Table 1, entry 4). From another point of view, the high aldehyde selectivity of the POC ligand indicated a high hydroformylation activity. The l/b ratio (0.99) of the PPh_3 ligand was lower than that of POC-DICP (l/b = 1.40, entry 3, Table 1), which suggests that our cage ligand exhibits high regioselectivity in hydroformylation. When the S/C value decreased from 12000 to 6000 (Table 1, entry 7), the aldehyde selectivity of the Rh/PPh_3 catalyst was improved slightly (71.4%), and the detrimental iso-alkene selectivity was reduced to 26.7%. However, the Rh/POC-DICP catalyst showed very good performance (Table 1, entry 6) under the same conditions as entry 6. The conversion and aldehyde selectivity were as high as 98.6% and 91.4%, respectively, the iso-alkane selectivity was only 7.8%, and the l/b ratio was as high as 1.88. We have also compared our catalyst to the Wilkinson-type catalyst (Table 1, entry 5). The results showed that the performance of our catalyst greatly exceeded that of the Wilkinson catalyst. Although the conversion of the Wilkinson-type catalyst was high (99%), the major product was the detrimental iso-alkene (53.9%), and the alkane selectivity was also relatively high (14.8%). By comparing

Table 1
Hydroformylation of 1-octene employing different catalysts.

Entry	Cat.	Time (h)	S/C (× 1000)	Conv. (%)	Aldehyde sel.%	Alkane sel.%	Iso-alkene sel.%	TOF (h^{-1})	*l/b*
1	Rh/POC	1	12	97.8	59.8	2.8	37.4	7018	1.46
2	Rh/PPh_3	1	12	96.8	37.2	5.4	57.4	4321	0.99
3	Rh/POC	4	12	>99	88.9	2.6	8.5	2654	1.40
4	Rh/PPh_3	4	12	>99	53.3	5.2	41.6	1591	0.99
5	$HRh(CO)(PPh_3)_3$	4	12	>99	31.3	14.8	53.9	934	0.54
6	Rh/POC	4	6	>99	91.4	0.8	7.8	1364	1.88
7	Rh/PPh_3	4	6	>99	71.4	1.9	26.7	1066	1.10

[a] Reaction conditions: $Rh(CO)_2(acac)$ (0.384 mg), POC-DICP (13.8 mg), molar ratio of Rh/ligand = 1/10, H_2/CO = 1/1 (the initial pressure is 1.0 MPa), toluene (5 mL), 100 °C, 4 h, S/C = substrate/catalyst (molar ratio), $m_{1\text{-octene}}$ = 2 g (S/C = 12000), $m_{1\text{-octene}}$ = 1 g (S/C = 6000). TOF = [(S/C) × Conv. (%) × $Sel._{Aldehyde}$ (%)]/Time (h), l/b ratio = linear/branch ratio of aldehyde isomers.

the above experimental data, we can conclude that our homogeneous Rh/POC-DICP catalyst exhibited enhanced performance compared with the classical Rh/PPh_3 and Wilkinson-type catalysts. These catalysts are all based on the functional PPh_3 ligand; however, their specific structures are different. In addition, some reported catalysts are listed in Table 2, demonstrating that our Rh/POC-DICP catalyst displayed high activity and selectivity comparable with that of the Rh-metalated porous organic polymer catalyst [18].

The scope of the substrates was then examined (Table 3). The hydroformylation of 1-octene was investigated again (reaction time was prolonged as compared with those listed in Table 1), and similarly excellent performance was obtained (Table 3, entry 1). However, when the substrate was changed to 2-octene (an internal olefin), the conversion was reduced from 99.5% to 90.9%. Moreover, the l/b ratio decreased dramatically, which is a feature of internal olefins (Table 3, entry 2). When 1-hexene with a relatively short chain was tested, very satisfactory performance (99.9% conversion and 97.3% aldehyde selectivity) was obtained (Table 3, entry 3), and the case of 1-heptene was almost the same (Table 3, entry 4). We also tested our catalyst toward styrene, which is an aryl olefin. An excellent activity (99.6% conversion and 98.6% aldehyde selectivity) was obtained (Table 3, entry 5). Finally, the gas olefin propene was tested as a substrate, with the aldehyde selectivity reaching 99.4%, and the l/b ratio was 1.5 (Table 3, entry 6), which also suggested high activity and good regioselectivity. In addition, it is worth noting that all the terminal olefins tended to form linear aldehydes; that is, the linear-to-branch ratio was greater than one.

Why does our POC ligand exhibit higher activity and selectivity than classical PPh_3 ligands? This comparative advantage might be explained by the favorable electron and steric effects. Compared with PPh_3, the P center of POC-DICP is less basic; that is, it is a weaker σ-donor and a better π-acceptor than PPh_3, which can be evaluated by recording the infrared spectroscopy of the corresponding Ni-CO complexes [80]. The stretching vibration frequency of CO in complex POC-DICP-$Ni(CO)_3$ is higher than that of PPh_3-$Ni(CO)_3$ (Fig. 5, the nickel carbonyl complexes are very toxic and not easy to be obtained, to be safe, the DFT calculation was used to predict their Infrared spectra information), which clearly demonstrates the relatively electron-deficient property of the POC-DICP ligand. Judging from the viewpoint of the substituent effect, the same conclusion can be drawn. The imine bonds at the *para*-position of the P center are electron-withdrawing groups; therefore, the P of POC-DICP is less basic than that of PPh_3, which has no substituents. According to previous studies on hydroformylation [55,81], the less basic POC-DICP ligand forces carbon monoxide dissociation during the catalytic cycle, leading to a higher reaction rate.

In terms of the steric effect, the Talman cone angle, θ, is a well-recognized parameter that characterizes the size of monodentate phosphine [55,82,83]. The Talman cone angle is defined as the solid angle formed with the coordinated metal at the vertex (centered at a distance of 2.28 Å from the P atom) and the van der Waals radii of the outermost atoms at the perimeter of the cone. Based on this calculational model, we calculated the cone angle of POC-DICP and found that the value is greater than that of PPh_3 (Fig. 6), which quantitatively demonstrated the large steric effect of POC-DICP. In the homogeneous Rh-catalyzed hydroformylation process, the step of alkene insertion (also called alkene coordination) ultimately determines whether a linear aldehyde or branch aldehyde is formed [84].

Table 2
Comparison with other reported catalysts (substrate is 1-octene).

Entry	Catalyst	Conv. (%)	Aldehyde sel. (%)	TOF (h^{-1})	Ref.
1	Rh/POC-DICP	99.5	88.9	2654	—
2	Rh/dppe	99.5	52.3	416	[18]
3	$Rh(CO)_2acac$	98.8	50.1	396	[18]
4	Rh/POL-dppe	96.9	99.3	770	[18]

Table 3
Hydroformylation of diverse olefins employing Rh/POC-DICP catalyst.

Entry	Substrates	Conv. (%)	Selectivity (%)			l/b
			Aldehydes	Alkane	Iso-alkenes	
1	1-octene	99.5	94.0	1.3	4.7	1.07
2	2-octene	90.9	89.8	3.2	7.0	0.17
3	1-hexene	99.9	97.3	0.5	2.2	1.89
4	1-heptene	95.0	94.0	0.9	5.1	1.39
5	Styrene	99.6	98.6	1.4	0	1.29
6 [a]	Propene	95.3	99.4	less	none	1.5

Reaction conditions: $Rh(CO)_2(acac)$ (0.384 mg), POC-DICP (13.8 mg), molar ratio of Rh/ligand = 1/10, H_2/CO = 1/1 (initial pressure is 1.0 MPa), toluene (5 mL), 100 °C, 12 h, S/C = 12000. [a] $C_3H_6/H_2/CO$ = 1/1/1 (initial pressure is 1.5 MPa).

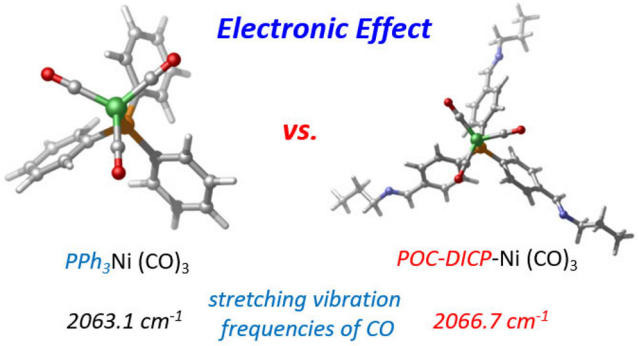

Fig. 5. IR diagrams of the complexes POC-DICP-Ni(CO)$_3$ and PPh$_3$-Ni(CO)$_3$.

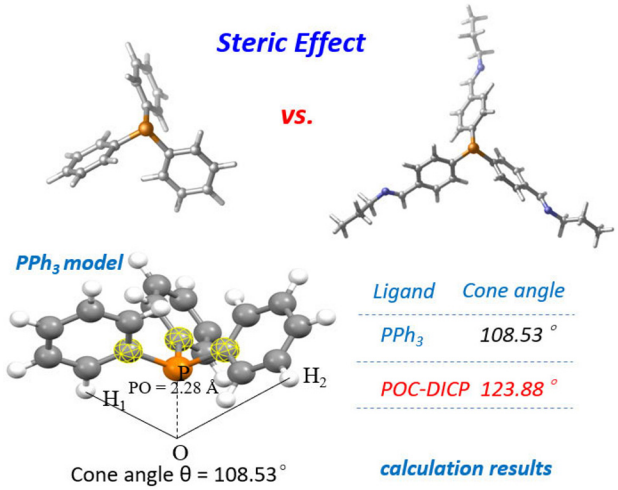

Fig. 6. Cone angles of POC-DICP and PPh$_3$.

The configuration in which the olefin is inserted is related to how crowded the space around Rh is. If the ligand has a strong steric effect, it will make the central Rh atom more crowded, providing a favorable configuration for the generation of a linear aldehyde during olefin insertion. Therefore, qualitatively, under the same coordination mode, the crowded POC-DICP ligand with a larger Talman cone angle is more favorable for the generation of a linear aldehyde than PPh$_3$.

To gain further insight into this selectivity advantage, a more accurate coordination status of the central Rh atom should be determined; thus, Rh K-edge EXAFS spectra were applied to investigate the coordination information. The pre-catalyst, which was used as a sample for the EXAFS test, was synthesized by the coordination reaction between POC-DICP, Rh(CO)$_2$(acac), and syngas (CO/H$_2$ = 1:1) under the standard reaction conditions (see Supporting Information). As shown in Fig. 7, when the number of P atoms coordinated with rhodium was set to approximately 1.6, the fitting result was optimal, which suggests that each Rh atom coordinated with 1.6 P atoms on average. With a simple arithmetical operation, we know that approximately 60% of Rh exhibits a dual P coordination mode and 40% of Rh exhibits a single P coordination mode (Fig. 7). The steric effect of the cage ligand is already large; thus, we expect the steric hindrance of the dual P coordination mode to be even greater owing to the "multiplier effect". Therefore, it is a preferential configuration for the formation of linear aldehyde, and the linear-to-branch ratio clearly should be greater than one under the 60% mode of dual P coordination.

However, it is difficult to predict the impact of the remaining 40% on the l/b ratio owing to the single P coordination mode. Scientific experience alone makes it difficult to reliably predict the impact of the single P coordination mode on selectivity. Hence, in this case, DFT calculations were used to investigate the mechanism of selectivity control (Fig. 8). Propene, rather than other long-chain olefins, was chosen as the substrate (to reduce unnecessary calculation). As illustrated in Fig. 8, two different paths, one representing the linear aldehyde path and the other representing the branch aldehyde path, were calculated. Consistent with the well-recognized hydroformylation mechanism, the first step is alkene coordination, whereas the second step is the isomerization step, which determines whether the linear aldehyde or the branch aldehyde is predominant. The entire catalytic cycle is illustrated in Fig. 9. According to the present DFT calculations, isomerization is an endothermic step (ΔE_{branch} = 14.45 and ΔE_{linear} = 11.90 kJ·mol^{-1}), which also indicates that this step is a rate-determining step. From the viewpoint of kinetics, the energy difference (14.45−11.9 = 2.55 kJ·mol^{-1}) is favorable for the generation of linear aldehyde; thus, even for the 40% single P

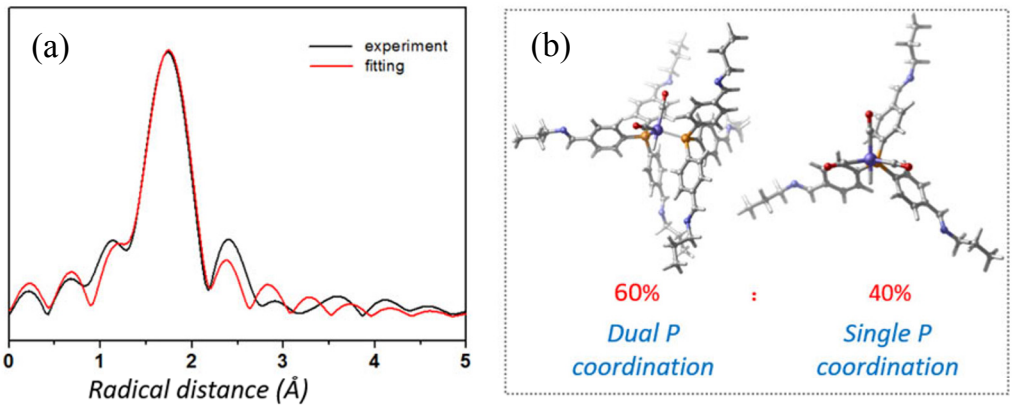

Fig. 7. EXAFS fitting spectra (a) and its corresponding interpretation of coordination modes (b).

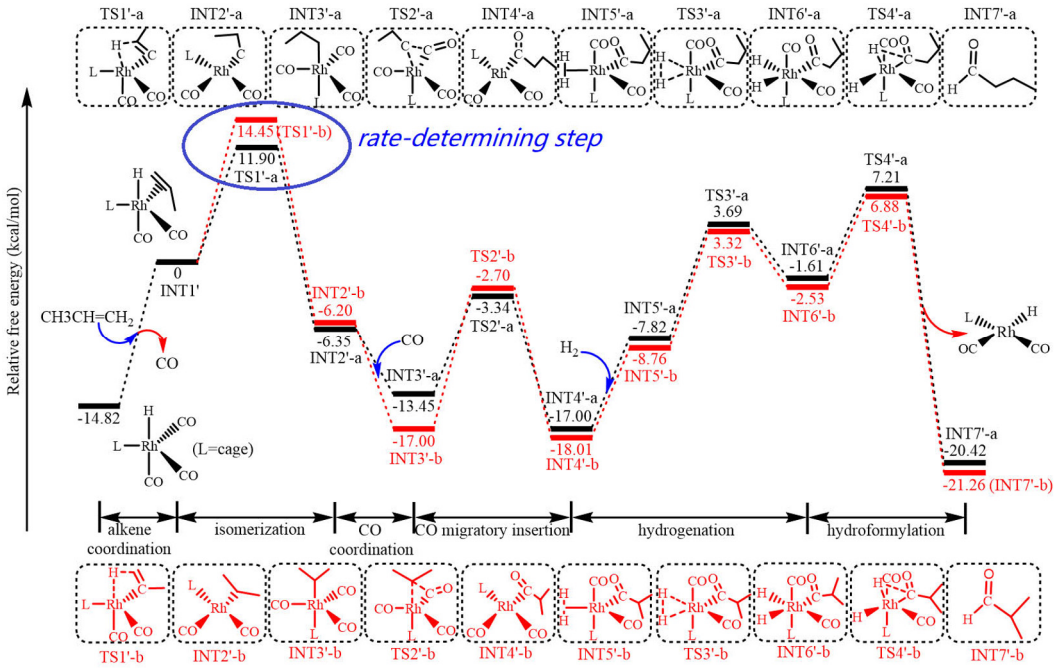

Fig. 8. Transition states of Rh-catalyzed hydroformylation reaction, and the energy comparison diagrams of two parallel paths of linear and branch aldehydes.

coordination state, linear aldehyde is preferential in energy. Together with the previous discussion of the 60% dual P coordination mode, we can conclude that the linear-to-branch ratio of aldehydes should be greater than one from a statistical point of view.

3.4. Catalyst recycling and reuse

A critical point in the hydroformylation mechanism is the separation of the catalyst and product. It is worth noting that the cage molecule, POC-DICP, was connected by six imine bonds, and we found that organic compounds containing imine bonds are generally very hard to solubilize in methanol; the same applies to the imine cages. This suggests a strategy—homogeneous catalysis and heterogeneous separation—for easy separation and recycling of the catalyst. When the homogeneous catalytic reaction was completed, methanol was added to precipitate the catalyst, and the catalyst was recycled by centrifugation or simple filtration. The recycled catalyst can be reloaded for the next run, and there is no clear loss of selectivity or activity by the fifth run (see Supporting Information). Analysis of the aqueous reaction solution after each cycle by ICP-AES shows that Rh element leaching did not reach the detection limit. We believe that the Rh/POC-DICP catalytic system provides a new idea for the catalyst recycling of homogeneous hydroformylation reactions, which might have important impacts, both in academia and industry.

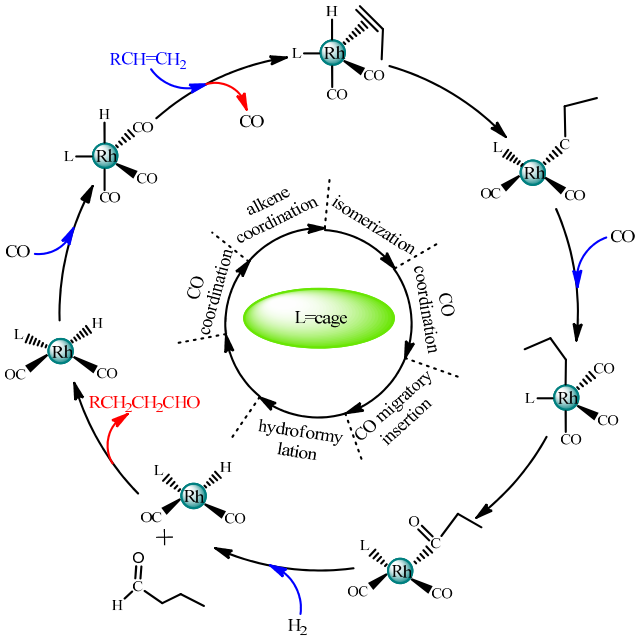

Fig. 9. Proposed hydroformylation cycle of linear aldehyde catalyzed by a single P cage-coordinated Rh catalyst.

Table 4
Catalyst recycling data of hydroformylation reaction.

Reaction cycle	Conversion (%)	Aldehydes sel. (%)	Alkane sel. (%)	Iso-alkenes sel. (%)	l/b ratio
1	99.6	85.4	6.1	8.5	1.38
2	99.6	85.1	6.2	8.7	1.41
3	99.6	86.0	5.8	8.2	1.40
4	99.6	86.1	5.8	8.1	1.40
5	99.6	85.9	5.9	8.2	1.43

Reaction conditions: $Rh(CO)_2(acac)$ (0.384 mg), POC-DICP (13.8 mg), molar ratio of Rh/ligand = 1/10, H_2/CO = 1/1 (initial pressure is 1.0 MPa), toluene (5 mL), 100 °C, 4 h, S/C = substrate/catalyst (molar ratio), $m_{1\text{-octene}}$ = 2 g (S/C = 12000), l/b ratio = linear/branch ratio of aldehyde isomers.

Graphical Abstract

Chin. J. Catal., 2021, 42: 1216–1226 doi: 10.1016/S1872-2067(20)63746-9

Enhancing the activity, selectivity, and recyclability of Rh/PPh_3 system-catalyzed hydroformylation reactions through the development of a PPh_3-derived quasi-porous organic cage as a ligand

Wenlong Wang, Cunyao Li, Heng Zhang, Jiangwei Zhang, Lanlu Lu, Zheng Jiang, Lifeng Cui, Hongguang Liu *, Li Yan *, Yunjie Ding *
Dalian Institute of Chemical Physics, Chinese Academy of Sciences;
Dongguan university of Technology;
Jinan University;
Shanghai Advanced Research Institute, Chinese Academy of Sciences;
Shanghai Institute of Applied Physics, Chinese Academy of Sciences

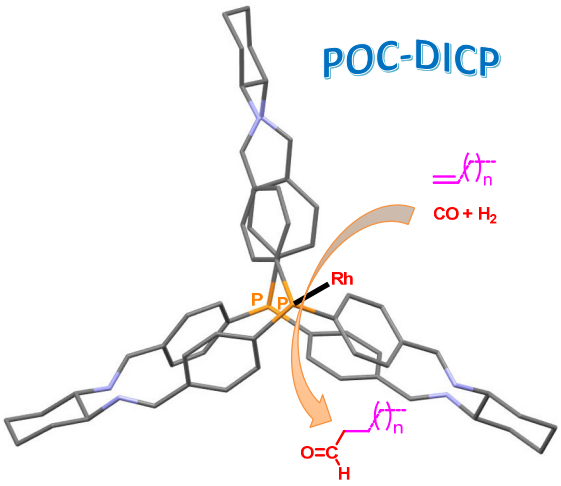

A PPh_3-derived porous organic cage (POC-DICP) was applied as an efficient and recyclable organic molecular cage ligand for Rh-catalyzed homogeneous hydroformylation reactions.

4. Conclusions

In conclusion, a novel PPh_3-functionalized porous organic cage, POC-DICP, has been successfully synthesized through the use of "dynamic covalent chemistry", which could be applied as an efficient ligand in the area of homogeneous hydroformylation reactions. Because of the multiple imine bond connections of POC-DICP, the Rh/POC-DICP catalyst could be recycled through the use of "homogeneous catalysis and heterogeneous separation" and reused several times without loss of selectivity or activity. This represents important progress after the ligand TPPTS and stimulates further development in this field. More importantly, compared with the classical PPh_3 ligand, POC-DICP exhibited enhanced hydroformylation activity and selectivity. The investigation of the structure-property relationship together with DFT calculations were employed to explain why POC-DICP performs better than PPh_3 in terms of hydroformylation reactions. The conclusion is that POC-DICP exhibits excellent electronic and steric effects that PPh_3 does not. The strategy of evolving from small organic molecule ligand (PPh_3) to cage ligand (POC-DICP) opens a wide range of applications for homogeneous catalysis, in which continuous improvement of activity and selectivity is required. Efforts towards the synthesis and understanding of other interesting and useful POC-based catalytic materials are currently in progress in our laboratory.

Electronic supporting information

Supporting information is available in the online version of this article.

References

[1] A. G. Slater, A. I. Cooper, *Science*, **2015**, 348, aaa8075.
[2] M. Zhao, K. Yuan, Y. Wang, G. Li, J. Guo, L. Gu, W. Hu, H. Zhao, Z. Tang, *Nature*, **2016**, 539, 76–80.
[3] L. Zhu, X.-Q. Liu, H.-L. Jiang, L.-B. Sun, *Chem. Rev.,* **2017**, 117, 8129–8176.
[4] A. Corma, H. Garcia, F. X. L. I. Llabres i Xamena, *Chem. Rev.,* **2010**, 110, 4606–4655.
[5] Q. Wang, D. Astruc, *Chem. Rev.,* **2020**, 120, 1438–1511.
[6] D. Liu, Z.-G. Ren, H.-X. Li, J.-P. Lang, N.-Y. Li, B. F. Abrahams, *Angew. Chem. Int. Ed.,* **2010**, 49, 4767–4770.
[7] F.-L. Hu, Y. Mi, C. Zhu, B. F. Abrahams, P. Braunstein, J.-P. Lang, *Angew. Chem. Int. Ed.,* **2018**, 57, 12696–12701.
[8] Y. Xiao, X. Guo, J. Liu, L. Liu, F. Zhang, C. Li, *Chin. J. Catal.,* **2019**, 40, 1339–1344.
[9] X. Feng, X. Ding, D. Jiang, *Chem. Soc. Rev.,* **2012**, 41, 6010–6022.
[10] S.-Y. Ding, W. Wang, *Chem. Soc. Rev.,* **2013,** 42, 548–568.
[11] S. M. J. Rogge, A. Bavykina, J. Hajek, H. Garcia, A. I. Olivos-Suarez, A. Sepulveda-Escribano, A. Vimont, G. Clet, P. Bazin, F. Kapteijn, M. Daturi, E. V. Ramos-Fernandez, F. X. Llabres i Xamena, V. Van Speybroeck, J. Gascon, *Chem. Soc. Rev.,* **2017**, 46, 3134–3184.
[12] X. Y. Guan, F. Q. Chen, Q. R. Fang, S. L. Qiu, *Chem. Soc. Rev.,* **2020**, 49, 1357–1384.
[13] C. Li, Y. Ma, H. Liu, L. Tao, Y. Ren, X. Chen, H. Li, Q. Yang, *Chin. J. Catal.,* **2020**, 41, 1288–1297.
[14] P. Kaur, J. T. Hupp, S. T. Nguyen, *ACS Catal.,* **2011**, 1, 819–835.
[15] S. Kramer, N. R. Bennedsen, S. Kegnaes, *ACS Catal.,* **2018**, 8, 6961–6982.
[16] L. Tan, B. Tan, *Chem. Soc. Rev.,* **2017**, 46, 3322–3356.
[17] Q. Sun, Z. Dai, X. Meng, F.-S. Xiao, *Chem. Soc. Rev.,* **2015**, 44, 6018–6034.
[18] Q. Sun, Z. Dai, X. Liu, N. Sheng, F. Deng, X. Meng, F.-S. Xiao, *J. Am. Chem. Soc.,* **2015**, 137, 5204–5209.
[19] W. Wang, C. Li, L. Yan, Y. Wang, M. Jiang, Y. Ding, *ACS Catal.,* **2016**, 6, 6091–6100.
[20] Y. Zhang, Y. Lyu, Y. Wang, C. Li, M. Jiang, Y. Ding, *Chin. J. Catal.,* **2019**, 40, 147–151.
[21] T. Tozawa, J. T. A. Jones, S. I. Swamy, S. Jiang, D. J. Adams, S. Shake-

speare, R. Clowes, D. Bradshaw, T. Hasell, S. Y. Chong, C. Tang, S. Thompson, J. Parker, A. Trewin, J. Bacsa, A. M. Z. Slawin, A. Steiner, A. I. Cooper, *Nat. Mater.,* **2009**, 8, 973–978.
[22] T. Hasell, A. I. Cooper, *Nat. Rev. Mater.,* **2016**, 1, 16053.
[23] J. R. Holst, A. Trewin, A. I. Cooper, *Nat. Chem.,* **2010**, 2, 915–920.
[24] T. Hasell, X. Wu, J. T. A. Jones, J. Bacsa, A. Steiner, T. Mitra, A. Trewin, D. J. Adams, A. I. Cooper, *Nat. Chem.,* **2010**, 2, 750–755.
[25] A. I. Cooper, *ACS Central Sci.,* **2017**, 3, 544–553.
[26] M. E. Briggs, A. I. Cooper, *Chem. Mater.,* **2017**, 29, 149–157.
[27] G. Zhang, O. Presly, F. White, I. M. Oppel, M. Mastalerz, *Angew. Chem. Int. Ed.,* **2014**, 53, 1516–1520.
[28] K. E. Jelfs, X. Wu, M. Schmidtmann, J. T. A. Jones, J. E. Warren, D. J. Adams, A. I. Cooper, *Angew. Chem. Int. Ed.,* **2011**, 50, 10653–10656.
[29] S. Jiang, J. T. A. Jones, T. Hasell, C. E. Blythe, D. J. Adams, A. Trewin, A. I. Cooper, *Nat. Commun.,* **2011**, 2, 207.
[30] E. Berardo, L. Turcani, M. Miklitz, K. E. Jelfs, *Chem. Sci.,* **2018**, 9, 8513–8527.
[31] V. Santolini, M. Miklitz, E. Berardo, K. E. Jelfs, *Nanoscale*, **2017**, 9, 5280–5298.
[32] R. Greenaway, V. Santolini, M. J. Bennison, B. M. Alston, C. J. Pugh, M. A. Little, M. Miklitz, E. G. B. Eden-Rumps, R. Clowes, A. Shakil, H. J. Cuthbertson, H. Armstrong, M. E. Briggs, K. E. Jelfs, A. I. Cooper, *Nat. Commun.,* **2018**, 9, 2849.
[33] J. T. A. Jones, T. Hasell, X. Wu, J. Bacsa, K. E. Jelfs, M. Schmidtmann, S. Y. Chong, D. J. Adams, A. Trewin, F. Schiffman, F. Cora, B. Slater, A. Steiner, G. M. Day, A. I. Cooper, *Nature,* **2011**, 474, 367–371.
[34] P. T. Smith, B. P. Benke, Z. Cao, Y. Kim, E. M. Nichols, K. Kim, C. J. Chang, *Angew. Chem. Int. Ed.,* **2018,** 57, 9684–9688.
[35] S. Hong, M. R. Rohman, J. Jia, Y. Kim, D. Moon, Y. Kim, Y. H. Ko, E. Lee, K. Kim, *Angew. Chem. Int. Ed.,* **2015**, 54, 13241–13244.
[36] X. Yang, J.-K. Sun, M. Kitta, H. Pang, Q. Xu, *Nat. Catal.,* **2018**, 1, 214–220.
[37] J.-K. Sun, W.-W. Zhan, T. Akita, Q. Xu, *J. Am. Chem. Soc.,* **2015**, 137, 7063–7066.
[38] Q. Song, W. D. Wang, X. Hu, Z. Dong, *Nanoscale*, **2019**, 11, 21513–21521.
[39] Y. Zhang, Y. Xiong, J. Ge, R. Lin, C. Chen, Q. Peng, D. Wang, Y. Li, *Chem. Commun.,* **2018**, 54, 2796–2799.
[40] B. Mondal, K. Acharyya, P. Howlader, P. S. Mukherjee, *J. Am. Chem. Soc.,* **2016**, 138, 1709–1716.
[41] S. Jiang, H. J. Cox, E. I. Papaioannou, C. Tang, H. Liu, B. J. Murdoch, E. K. Gibson, I. S. Metcalfe, J. S. O. Evans, S. K. Beaumont, *Nanoscale*, **2019**, 11, 14929–14936.
[42] N. Giri, M. G. Del Popolo, G. Melaugh, R. L. Greenaway, K. Raetzke, T. Koschine, L. Pison, M. F. C. Gomes, A. I. Cooper, S. L. James, *Nature*, **2015**, 527, 216–220.
[43] A. U. Malik, F. Gan, C. Shen, N. Yu, R. Wang, J. Crassous, M. Shu, H. Qiu, *J. Am. Chem. Soc.,* **2018**, 140, 2769–2772.
[44] Z. Wang, H. Ma, T.-L. Zhai, G. Cheng, Q. Xu, J.-M. Liu, J. Yang, Q.-M. Zhang, Q.-P. Zhang, Y.-S. Zheng, B. Tan, C. Zhang, *Adv. Sci.,* **2018**, 5 1800141.
[45] M. Liu, L. Chen, S. Lewis, S. Y. Chong, M. A. Little, T. Hasell, I. M. Aldous, C. M. Brown, M. W. Smith, C. A. Morrison, L. J. Hardwick, A. I. Cooper, *Nat. Commun.,* **2016**, 7, 12750.
[46] Y. Jin, B. A. Voss, A. Jin, H. Long, R. D. Noble, W. Zhang, *J. Am. Chem. Soc.,* **2011**, 133, 6650–6658.
[47] P. S. Reiss, M. A. Little, V. Santolini, S. Y. Chong, T. Hasell, K. E. Jelfs, M. E. Briggs, A. I. Cooper, *Chem. - Eur. J.,* **2016**, 22, 16547–16553.
[48] Y. Li, H. Wang, C. Wang, J. Xu, S. Ma, J. Ou, J. Zhang, G. Li, Y. Wei, M. Ye, *ACS Appl. Mater. Interfaces*, **2020**, 12, 17827–17835.
[49] H.-X. Li, T.-P. Xie, K.-Q. Yan, S.-M. Xie, B.-J. Wang, J.-H. Zhang, L.-M. Yuan, *Microchim. Acta,* **2020**, 187, 269.
[50] M. Brutschy, M. W. Schneider, M. Mastalerz, S. R. Waldvogel, *Chem. Commun.,* **2013**, 49, 8398–8400.
[51] M. Brutschy, M. W. Schneider, M. Mastalerz, S. R. Waldvogel, *Adv. Mater.,* **2012**, 24, 6049–6052.
[52] M. Mastalerz, M. W. Schneider, I. M. Oppel, O. Presly, *Angew. Chem. Int. Ed.,* **2011**, 50, 1046–1051.
[53] A. Börner, R. Franke, Hydroformylation: Fundamentals, Processes, and Applications in Organic Synthesis, Wiley-VCH, Weinheim, **2016**.
[54] M. Beller, *Catalytic Carbonylation Reactions*, Springer, Berlin, **2006**.
[55] R. Franke, D. Selent, A. Boerner, *Chem. Rev.,* **2012**, 112, 5675–5732.
[56] F. Hebrard, P. Kalck, *Chem. Rev.,* **2009**, 109, 4272–4282.
[57] M. Vilches-Herrera, L. Domke, A. Boerner, *ACS Catal.,* **2014**, 4, 1706–1724.
[58] H. Tricas, O. Diebolt, P. W. N. M. van Leeuwen, *J. Catal.,* **2013**, 298, 198–205.
[59] J. Zhang, P. Sun, G. Gao, J. Wang, Z. Zhao, Y. Muhammad, F. Li, *J. Catal.,* **2020**, 387, 196–206.
[60] D. M. Hood, R. A. Johnson, A. E. Carpenter, J. M. Younker, D. J. Vinyard, G. G. Stanley, *Scienc*e, **2020**, 367, 542–548.
[61] *Chem. Abstr.,* **1944**, 38, 3631.
[62] J. A. Osborn, G. Wilkinson, *Inorg. Synth.,* **1967**, 10, 67–71.
[63] V. I. Zapirtan, B. L. Mojet, J. G. van Ommen, J. Spitzer, L. Lefferts, *Catal. Lett.,* **2005**, 101, 43–47.
[64] S. K. Sharma, R. V. Jasra, *Catal. Today*, **2015**, 247, 70–81.
[65] B. Cornils, E. G. Kuntz, *J. Organomet. Chem.,* **1995**, 502, 177–186.
[66] C. W. Kohlpaintner, R. W. Fischer, B. Cornils, *Appl. Catal. A,* **2001**, 221, 219–225.
[67] Q. Sun, M. Jiang, Z. Shen, Y. Jin, S. Pan, L. Wang, X. Meng, W. Chen, Y. Ding, J. Li, F.-S. Xiao, *Chem. Commun.,* **2014**, 50, 11844–11847.
[68] M. Jiang, L. Yan, Y. Ding, Q. Sun, J. Liu, H. Zhu, R. Lin, F. Xiao, Z. Jiang, J. Liu, *J. Mol. Catal. A*, **2015**, 404, 211–217.
[69] C. Li, L. Yan, L. Lu, K. Xiong, W. Wang, M. Jiang, J. Liu, X. Song, Z. Zhan, Z. Jiang, Y. Ding, *Green Chem.,* **2016**, 18, 2995–3005.
[70] Y. Wang, L. Yan, C. Li, M. Jiang, W. Wang, Y. Ding, *Appl. Catal. A*, **2018**, 551, 98–105.
[71] C. Li, K. Xiong, L. Yan, M. Jiang, X. Song, T. Wang, X. Chen, Z. Zhan, Y. Ding, *Catal. Sci. Technol.,* **2016**, 6, 2143–2149.
[72] T. Wang, W. Wang, Y. Lyu, K. Xiong, C. Li, H. Zhang, Z. Zhan, Z. Jiang, Y. Ding, *Chin. J. Catal.,* **2017**, 38, 691–698.
[73] C. Li, K. Sun, W. Wang, L. Yan, X. Sun, Y. Wang, K. Xiong, Z. Zhan, Z. Jiang, Y. Ding, *J. Catal.,* **2017**, 353, 123–132.
[74] Y. Wang, L. Yan, C. Li, M. Jiang, Z. Zhao, G. Hou, Y. Ding, *J. Catal.,* **2018**, 368, 197–206.
[75] W. Wang, L. Cui, P. Sun, L. Shi, C. Yue, F. Li, *Chem. Rev.,* **2018**, 118, 9843–9929.
[76] P. A. Bartiett, B. Bauer, S. J. Singer, *J. Am. Chem. Soc.,* **1978**, 100, 5085–5089.
[77] A. V. Marenich, C. J. Cramer, D. G. Truhlar, *J. Phys. Chem. B*, **2009**, 113, 6378–6396.
[78] A. W. Ehlers, M. Böhme, S. Dapprich, A. Gobbi, A. Höllwarth, V. Jonas, K. F. Köhler, R. Stegmann, A. Veldkamp, G. Frenking, *Chem. Phy. Lett.,* **1993**, 208, 111–114.
[79] S. Grimme, J. Antony, S. Ehrlich, H. Krieg, *J. Chem. Phys.,* **2010**, 132, 154104.
[80] O. Kühl, *Coord. Chem. Rev.,* **2005**, 249, 693–704.
[81] O. Diebolt, H. Tricas, Z. Freixa, P. W. N. M. van Leeuwen, *ACS Catal.,* **2013**, 3 128–137.

[82] C. A. Tolman, *J. Am. Chem. Soc.*, **1970**, 92, 2956–2965.
[83] C. A. Tolman, *Chem. Rev.*, **1977**, 77, 313–348.
[84] P. Dydio, R. J. Detz, J. N. H. Reek, *J. Am. Chem. Soc.*, **2013**, 135, 10817–10828.

PPh_3衍生准多孔有机笼在Rh/PPh_3体系催化氢甲酰化反应中的应用: 增强活性和选择性及可回收利用

汪文龙[b,†], 李存耀[a,†], 张 恒[c,†], 张江威[a], 卢兰露[d], 姜 政[d,e], 崔立峰[b], 刘宏光[c,#], 严 丽[a,$], 丁云杰[a,*]

[a]中国科学院大连化学物理研究所, 洁净能源国家实验室(筹), 催化基础国家重点实验室, 辽宁大连116023
[b]东莞理工学院材料科学与工程学院, 广东东莞523808
[c]暨南大学化学与材料学院, 广东暨南510632
[d]中国科学院上海高等研究院, 上海210210
[e]中国科学院上海应用物理研究所, 上海同步辐射光源, 上海201204

摘要: 多孔有机笼(POCs)由英国利物浦大学的Cooper教授在2009年首次合成, 这种多孔小分子材料的出现具有两方面重要意义: (1)开拓了多孔材料领域的一个全新分支, 改变了人们对多孔材料的传统认知; (2)由于POCs材料由离散的小分子堆积而成, 可溶解于一些常用的有机溶剂中, 因此其在材料制备方面具有很好的"溶液成型"性能, 该优势是三维延伸网状多孔材料所不具备的. POCs本质上是一种"中心带孔"的有机小分子, 由刚性有机分子砌块收敛堆叠而成, 其特殊结构在气体吸附与分离等方面表现出很好的应用前景. 不同于传统空间延伸网状框架材料(如金属-有机框架材料和共价有机框架材料)及多孔有机聚合物(POPs)材料, POCs是一种在大多数有机溶剂中可溶解的小分子材料, 因此在均相催化领域也有很好的应用前景.

作为最为经典的有机配体, 三苯基膦(PPh_3)在金属有机化学和均相催化领域应用十分广泛, 如目前均相催化工业应用最成功的典范之一氢甲酰化反应, 大多数情况下使用的是PPh_3与Rh形成的络合物催化剂. 本文首先将PPh_3进行醛基官能团化, 通过醛基和氨基的收敛缩合形成POCs材料, 合成了基于PPh_3配体的准多孔有机笼(POC-DICP), 利用得到的多孔有机笼制备出类Rh/PPh_3均相催化体系的Rh/POC-DICP络合催化体系, 并将其应用于氢甲酰化反应. 相比于经典的Rh/PPh_3均相催化体系, 该Rh/POC-DICP催化体系在氢甲酰化反应中不仅展示出了更高的活性和目标产物醛的选择性(醛的化学选择性为97%, 醛的正异构比为1.89), 而且可以很方便地从均相反应体系中沉淀回收(通过调整溶剂体系极性). 在氢甲酰化反应中, Rh/POC-DICP体系显示出了良好的底物适用性, 在己烯、庚烯、辛烯和苯乙烯的氢甲酰化反应中均表现出良好的催化活性和醛选择性, 同时催化剂回收使用4次, 未见催化性能明显下降. X射线单晶衍射、同步辐射及DFT计算等结果表明, Rh/POC-DICP催化体系在氢甲酰化反应中具有较高活性和选择性的原因是POC-DICP多孔有机笼分子的有利的空间咬合角(123.88°)和P原子上相对的缺电子效应.

本文设计合成的PPh_3衍生的多孔有机笼不仅拓宽了多孔有机笼材料在催化领域的应用, 而且为新型配体及络合催化剂的设计、合成及修饰提供了新的思路.

关键词: 氢甲酰化反应; 三苯基膦; 多孔有机笼; 化学选择性; 线性-区域选择性

收稿日期: 2020-10-22. 接受日期: 2020-11-25. 上网时间: 2021-03-05.
*通讯联系人. 电话/传真: (0411)84379143; 电子信箱: dyj@dicp.ac.cn
#通讯联系人. 电话: 15602302185; 电子信箱: hongguang_liu@jnu.edu.cn
$通讯联系人. 电话: (0411)84379143; 电子信箱: yanli@dicp.ac.cn
†共同第一作者.
基金来源: 中国科学院战略性先导科技专项(XDA21020300, XDB17020400); 国家重点研发计划(2017YFB0602203); 国家自然科学基金(21972018); 东莞理工学院新能源材料研究中心(KCYCXPT2017005); 东莞理工学院科研启动基金(KCYKYQD2017015).
本文的电子版全文由Elsevier出版社在ScienceDirect上出版(http://www.sciencedirect.com/journal/chinese-journal-of-catalysis).